1958 *Inorg. Chem.* **1990,** *29,* 1958-1967

Contribution from the Departments of Chemistry, Grinnell College,
Grinnell, Iowa 50112, and Fairfield University, Fairfield, Connecticut 06430

Multinuclear NMR Studies of Platinum(IV) Complexes. 1. Acid Dissociation, Anation, and Intramolecular Catalysis of Bipyridyl Proton Exchange in [Aqua(bipyridine)(1,3,5-triaminocyclohexane)platinum(IV)](4+)

Luther E. Erickson,*[†] David J. Cook,[†] Gregory D. Evans,[†] Joseph E. Sarneski,*[‡] Paul J. Okarma,[‡] and Anthony D. Sabatelli[‡]

Received August 28, 1989

Nuclear magnetic resonance (^1H, ^{13}C, and ^{195}Pt) and UV spectral measurements were employed to establish the protonation scheme of the potentially tetraprotic acid [aqua(bipyridine)(1,3,5-triaminocyclohexane)platinum(IV)](4+) cation (**2**). Three dissociation constants, corresponding to the H_2O and the two in-plane NH_2 moieties (with approximate pK_a values of −0.6, 5.5, and 11.7, respectively), were detected in the 1 M HCl to pH 13 range. The rate of deuterium exchange of H-6 protons of coordinated bpy in D_2O at pH 7–9 and in 0.05–0.20 M NaOD was found to be independent of pH, indicating an intramolecular catalysis of the process by electron pairs of deprotonated NH_2 groups of coordinated 1,3,5-triaminocyclohexane (tach). Qualitative conclusions about the preferred orientation of the lone pair(s) in the mid- and high-pH forms of **2** were derived from the NMR and kinetic data. The rate and extent of chloride anation of **2** in 0.2 M DCl was also determined.

Introduction

In 1977, we reported the synthesis and characterization by NMR spectroscopy, ESCA spectroscopy, and X-ray diffraction of a unique 6-coordinate platinum(IV) compound, containing coordinated bipyridine and *cis,cis*-1,3,5 triaminocyclohexane (tach).[1] On the basis of the analytical and X-ray data, the formula was determined to be $[Pt(bpy)(tach\text{-}2H)(H_2O)]Cl_2{\cdot}3H_2O$ (**1**) with the two in-plane coordinated nitrogens of the tach moiety deprotonated (hence denoted tach-2H) and the coordinated water fully protonated. The structure was of interest because of the facile loss of protons of coordinated tach and because of the unusually mild oxidation conditions that led to its formation by reaction of tach with $Pt(bpy)Cl_2$ in aqueous solution in a vessel open to the air. More recently Weighart et al. have reported another example of a platinum(II) complex that undergoes facile oxidation by molecular oxygen.[2]

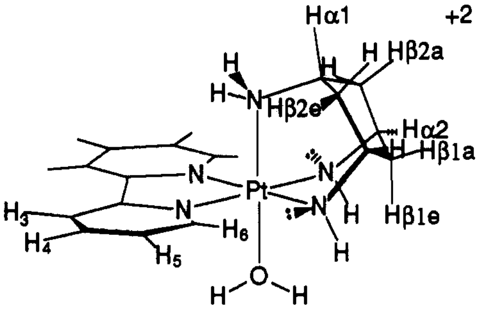

$[Pt(bpy)(tach\text{-}2H)(H_2O)]^{2+}$

1

After examining the acid–base and dimerization properties of some related monoaqua complexes of platinum(II),[3,4] we recognized that the coordinated water molecule of **1** would be too acidic to be protonated at mid-pH. We had also noted in our initial work that the H-6 protons of the bpy fragment of **1** exchanged relatively rapidly in D_2O at mid-pH, so we undertook a further study of the acid–base and proton-exchange properties of the compound. The study was undertaken to establish the details of the protonation scheme for the low pH form, a potentially tetraprotic acid (**2**) denoted $[Pt(bpy)(tach)(H_2O)]^{4+}$, which contains a coordinated water and three coordinated and fully protonated amine moieties. In particular, comparison with other Pt(IV) analogues, like $Pt(NH_3)_5(H_2O)^{4+}$ for which the pK_a for Pt–OH_2 equals 4.1,[5] and $Pt(NH_3)_6^{4+}$ whose pK_a = 7.9,[6,7] suggests that the coordinated water would be expected to be the most acidic site of **2** in aqueous solution, even though the X-ray data for **1** indicated that the two in-plane nitrogens are deprotonated in the solid state. In this structure, the two coordinated aminate groups are very different; one utilizes none of its hydrogen-bonding capability at all while the other forms two hydrogen bonds with the lone pair interacting with the coordinated water of a neighboring $[Pt(bpy)(tach\text{-}2H)(H_2O)]^{2+}$ in the crystal. Furthermore, the pH of a solution of $[Pt(bpy)(tach\text{-}2H)(H_2O)]Cl_2$, which contains a 2+ cation from the loss of two protons of $[Pt(bpy)(tach)(H_2O)]^{4+}$) is about 8, so two protonation sites must have pK_a values below 8.

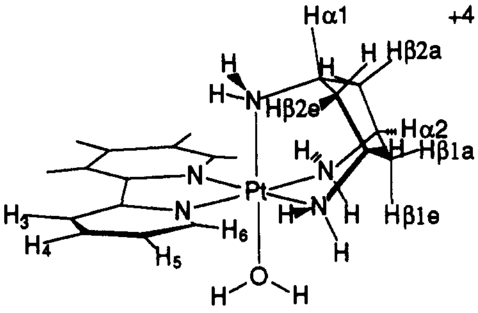

$[Pt(bpy)(tach)(H_2O)]^{4+}$

2

On the basis of NMR and UV spectral data over a wide pH range from 1 M HCl to 0.2 M NaOH, we have established that the stepwise dissociation of 2 is most accurately described by eq 1–3. Structures of the full range of species included in eq 1–3, including isomers resulting from removal of a specific amine proton

$$\underset{\mathbf{2}}{[Pt(bpy)(tach)(H_2O)]^{4+}} \xrightleftharpoons{K_{a1}} [Pt(bpy)(tach)(OH)]^{3+} + H^+ \tag{1}$$

$$\underset{\mathbf{3}}{[Pt(bpy)(tach)(OH)]^{3+}} \xrightleftharpoons{K_{a2}} \underset{\mathbf{4}}{[Pt(bpy)(tach\text{-}H)(OH)]^{2+}} + H^+ \tag{2}$$

$$\underset{\mathbf{4}}{[Pt(bpy)(tach\text{-}H)(OH)]^{2+}} \xrightarrow{K_{a3}} \underset{\mathbf{5}}{[Pt(bpy)(tach\text{-}2H)(OH)]^{+}} + H^+ \tag{3}$$

[†] Grinnell College.

[‡] Fairfield University.

(1) Sarneski, J. E.; McPhail, A. T.; Onan, K. D.; Erickson, L. E.; Reiley, C. N. *J. Am. Chem. Soc.* **1977**, *99*, 7376.

(2) Weighart, K.; Koppen, M.; Swiridoff, W.; Weiss, J. *J. Chem. Soc., Dalton Trans.* **1983**, 1869.

(3) Erickson, L. E.; Erickson, H. L.; Meyer, T. Y. *Inorg. Chem.* **1987**, *26*, 997.

(4) Erickson, L. E.; Burgeson, I. E.; Eidsmoe, E.; Larsen, R. G. *Inorg. Chem.* **1989**, *28*, 1315.

(5) Koshy, K. S.; Harris, G. M. *Inorg. Chem.* **1983**, *22*, 2947.

(6) Grinberg, A. A. *The Chemistry of Complex Compounds*; Pergamon Press: New York, 1962.

(7) Jørgensen, C. K. *Inorganic Complexes*; Academic Press: New York, 1963; p 59.

0020-1669/90/1329-1958$02.50/0

from **2**, are shown in Figure 1, structures **2**–**5**. The isomers of **4** and **5** are labeled by the prefixes eH, aH, etc. to denote the status of pairs of electrons on the two in-plane tach nitrogens: equatorial (e), axial (a), or protonated (H).

In investigating the effect of pH on the nmr spectrum of **1**, we noted—initially to our surprise—that the H-6 proton of the coordinated bpy undergoes a relatively facile proton exchange in D_2O under neutral and mildly basic conditions (pH 8–10). Reports of base-catalyzed H-3 proton exchange of coordinated bpy in DMSO-d_6/CD_3–OD or DMSO-d_6/D_2O solutions of tris(bipyridine) complexes of ruthenium[8] and osmium[9] encouraged us to examine more closely this bpy proton exchange of compound **1**. More recently, Constable has shown that both H-3 and H-6 undergo base-catalyzed exchange for the corresponding $[Rh(bpy)_3]^{3+}$.[10] However, unlike the tris(bipyridine) complexes of osmium, ruthenium, and rhodium, which show first-order dependence of exchange rates on free base in solution, the deprotonated forms of **2** have basic sites within the molecule that could permit intramolecular catalysis of exchange of favorably oriented bpy protons (H-6). Ultimately, kinetic data from the proton-exchange experiments confirmed the intramolecular catalysis and provided valuable evidence regarding the detailed stereochemistry of the 2+ and 1+ species, **4** and **5**, derived from **2** by the loss of two and three protons, respectively.

Experimental Section

Synthesis of 1. Compound **1** was prepared as described in our initial report[1] by heating, with stirring, a stoichiometric quantity of tach with a suspension of $[Pt(bpy)Cl_2]$ in water. After the $[Pt(bpy)Cl_2]$ dissolved to produce a yellow-orange solution, further heating and evaporation of solvent led to precipitation of compound **1**, which was purified by recrystallization from dioxide–water.

NMR Spectra. Proton, ^{13}C, and ^{195}Pt NMR spectra of solutions of **1** were obtained over a range of pH conditions at several different frequencies on four different NMR spectrometers (^1H = 250, 300, 270, and 500 MHz). All proton and ^{13}C chemical shifts were measured relative to internal standards (dioxane or *tert*-butyl alcohol), 1.25 ppm for *tert*-butyl protons and 67.73 ppm for dioxane carbons. Platinum-195 spectra were recorded at 64 MHz with a Bruker-IBM spectrometer (^1H at 300 MHz). Platinum-195 shifts were measured relative to external 0.2 M Na_2PtCl_6.

NMR Titrations. NMR titrations were carried out on solutions of 1 in D_2O or (for ^{13}C measurements) in 10% D_2O/H_2O mixtures. A 0.01–0.03 M solution (0.1 M for ^{13}C measurements) of **1** was prepared. After the spectrum was recorded, the sample was transferred to a small test tube, and the pH was determined with a conventional pH meter that had been standardized at pH 7 and 10 (for high pH samples) or pH 7 and 4 (for low pH samples). The standard buffer solutions were in H_2O solvent, so for D_2O solutions the pH electrode was rinsed once in a test tube of D_2O before insertion into the sample, in order to minimize the solvent water peak in the proton spectrum. The stock solution of **1** has a pH of about 8, so concentrated NaOD or DCl ($\approx$1 M) was then added in small increments to separate fractions to raise or lower the pH. A meter reading was recorded, the spectrum was recorded, and the pH measurement was repreated. Addition of base or acid was continued until changes in the spectra were no longer evident.

Platinum-195 chemical shifts of the variously protonated species were obtained by recording the spectra of a 0.05 M solution of **1** at a pH of about 8. Reference solutions at high pH and about pH 3 were then prepared by adding NaOD or DCl to separate portions of the stock solution. A separate sample was used to obtain the pH dependence of the ^{195}Pt chemical shifts at low pH. One milliliter of a 0.05 M solution in 1.2 M DCl was prepared and its spectrum recorded. The sample was then diluted in half to reduce the concentration of excess DCl to about 0.6 M, and another spectrum was recorded. To test for possible significant electrolyte concentration effects on ^{195}Pt shifts, the sample was the neutralized with NaOH to pH 3, rotary evaporated to dryness, and redissolved in D_2O. The Pt shift of **1** in this solution was essentially identical with the shift of a pH 1.6 reference solution that did not contain excess NaCl.

All NMR measurements were carried out at magnet temperature without regulation of the probe temperature; pH measurements were also done at room temperature, 22 ± 3 °C.

UV Spectra and Titrations. UV spectra of 5×10^{-5} M **1** in 1-cm quartz cells were obtained with a Beckman Model 5260 spectrophotometer for solutions in 0.10 M acetic acid/0.10 m sodium perchlorate (to maintain the ionic strength of 0.1; pH $\approx$3), 0.10 M sodium acetate (pH $\approx$9), and 0.10 M NaOH (pH $\approx$13) to establish the spectra of the three dominant species in the pH 2–13 range. Appropriate pairs of stock solutions were then mixed in varying ratios to obtain a series of solutions with identical total concentrations of **1** and ionic strength, but whose pHs spanned the pK_a of interest. Each solution was thermostated at 25 °C for both pH and UV spectral measurements. Several UV traces of the 250–400-nm range were overlayed on a single chart to reveal the spectral shift associated with the pH-dependent shift in species distribution.

Kinetics of H-6 Proton Exchange and Chloride Anation. Solutions for proton exchange and chloride anation were prepared by dissolving enough solid **1** to yield a 0.01–0.02 M solution in the appropriate solvent: high pH, 0.19 M NaOD; mid-pH, **1** alone; low pH, 0.18 M DCl. A low concentration (0.001 M) of *tert*-butyl alcohol was included in all of the solutions to serve as a chemical shift standard and as a potential reference peak for area measurements in the proton NMR spectrum. The solutions were transferred to NMR tubes and refrigerated except during the actual kinetic runs. Separate tubes were thermostated in water baths at 60, 45 and 25 °C. Under the conditions of the experiments, the exchange and anation reactions were slow enough to permit room-temperature data collection without serious error in the time.

Concentration–time data were derived from the NMR spectra, which are illustrated in Figures 2 and 3. At high pH, where the H-6 proton doublet is well-defined, the relative concentration of protonated species at each time was calculated from the ratio of the integrated areas of H-6 peaks to the sum of the areas of the other three bpy protons, which did not show any evidence of exchange. At mid pH, where the H-6 signal is very broad, the relative concentration was determined by comparing the H-6 and *tert*-butyl methyl peak heights, after processing the fid with a line broadening of 10 Hz.

At low pH in 0.18 M DCl, there was no evidence of H-6 proton exchange, but the spectrum showed a clean transition from the starting complex to a new species, presumed to be the chloride anation product $[Pt(bpy)(tach)Cl]^{3+}$, in which the principal differences lie in the chemical shifts of H-6 and of Hα2. The relative concentration of starting aqua species at each time was calculated from the ratio of peak height of the central doublet to the sum of the peak heights of the central doublets of the two species in the H-6 portion of the spectrum.

For both the H-6 proton exchange and the chloride anation, the concentration–time data were treated as first-order reactions by plotting ln (concentration) vs time to obtain k_1 as the slope or concentration vs time to obtain k by a nonlinear least-squares treatment. Such plots are illustrated for the high-pH exchange at all three temperatures in Figure 4 and for the low-pH chloride anation at 60 °C in Figure 5.

Computer. Numerical analysis and graphical presentation of the data were carried out with a VAX 8600 computer system using RS/1 software.

Results

Determination of pK_a Values: NMR Method for pK_{a2} and pK_{a3}. The proton and ^{13}C chemical shifts of **1** were determined at 15–20 pH values between pH 2 and 13. From both proton and carbon-13 data, it is clear that the greatest changes in shifts are observed near pH 5 and 12, which indicates pK_a values near 5 and 12. Since two of the potential protonation sites are deprotonated at pH 8, the two pK_a values that are revealed by these data should be identified as pK_{a2} and pK_{a3} of the potentially tetraprotic species **2**. With this great a difference between pK_a values, the separate steps in the protonation scheme can be treated individually. Though any proton or carbon signal could be used as the basis of a pK_a determination, more reliable values—as well as valuable clues regarding the isomer distribution of deprotonated species—can be obtained by examining the pH dependence of the shifts of all of the protons and carbons of the coordinated ligands.

For each determination, the chemical shift–pH data for a specific proton or carbon was divided into values below pH 8.5 and values above pH 8.5. Each of the sets of data was then analyzed by a least-squares fit of the three-parameter function

$$\delta = (f_{HA}\delta_{HA}) + (f_{A^-}\delta_{A^-}) \qquad (4)$$

where

$$f_{HA} = 10^{-pH}/[10^{-pH} + 10^{-pK_a}] \qquad (5)$$

and

---

(8) Constable, E. C.; Seddon, K. R. *J. Chem. Soc., Chem. Commun.* **1982**, 34.

(9) Wernberg, O. *J. Chem. Soc., Dalton Trans.* **1986**, 1993.

(10) Constable, E. C. *Polyhedron* **1989**, *8*, 83.

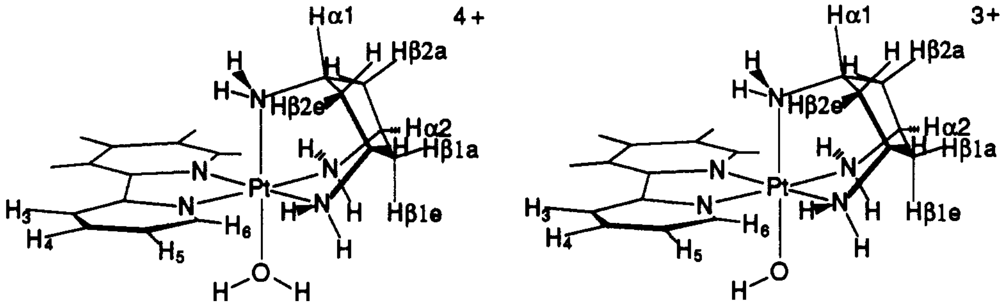

$[Pt(bipy)(tach)(H_2O)]^{4+}$ $[Pt(bipy)(tach)(OH)]^{3+}$

2 **3**

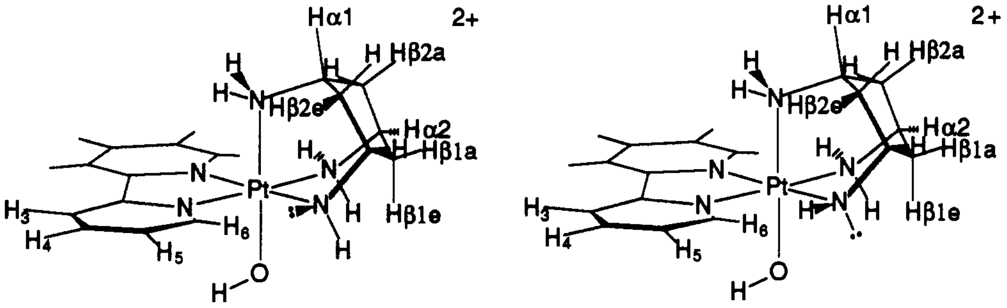

eH-$[Pt(bipy)(tach\text{-}H)(OH)]^{2+}$ aH-$[Pt(bipy)(tach\text{-}H)(OH)]^{2+}$

4eH **4aH**

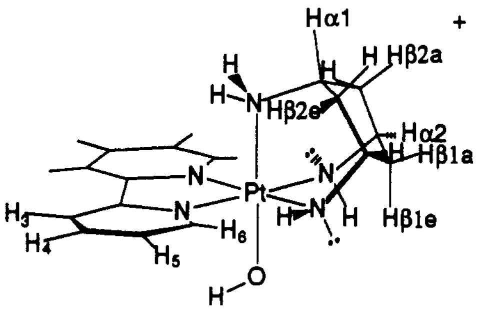

ae-$[Pt(bipy)(tach\text{-}2H)(OH)]^{+}$

5ae

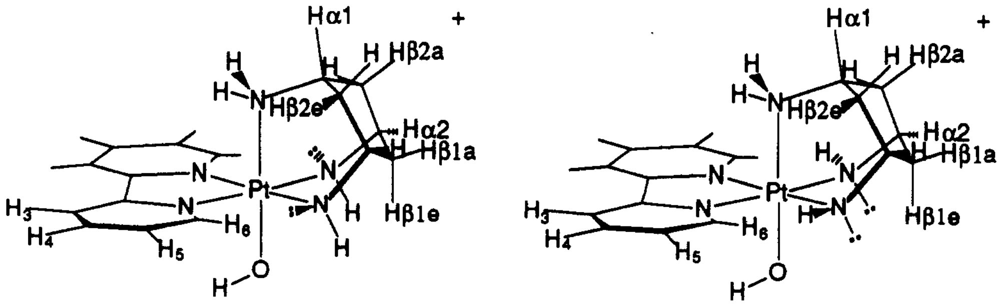

ee-$[Pt(bipy)(tach\text{-}2H)(OH)]^{+}$ aa-$[Pt(bipy)(tach\text{-}2H)(OH)]^{+}$

5ee **5aa**

Figure 1. Structures of $[Pt(bpy)(tach)(H_2O)]^{4+}$ (**2**) and the basic species **3**–**5** obtained from **2** by step-wise deprotonation. The notations eH, ae, etc. are used to describe the protonation state (H if fully protonated) or orientation of the lone pair (axial = e; equatorial = a) at in-plane tach nitrogen sites of **4** and **5**.

$$f_{A^-} = 10^{-pK_a}/[10^{-pH} + 10^{-pK_a}] \qquad (6)$$

to obtain the chemical shifts, δ_{HA} and δ_{A^-}, as well as pK_a and the standard deviations in each of the three quantities. Low-pH data yielded $\delta(3+)$ and $\delta(2+)$; high-pH data gave $\delta(2+)$ and $\delta(1+)$, where the charge represents the charge on successive conjugate base species derived from the tetraprotic (4+) species [Pt(bpy)(tach)(H_2O)]$^{4+}$. The chemical shift values are collected in Table I. The values given for $\delta(2+)$ are averages of the separate (but nearly identical) values obtained from the separate determinations of pK_{a2} and pK_{a3}. The 4+ species was too acidic to obtain reliable values for its chemical shifts under the conditions employed. Average pK_a values derived from the analysis are listed in Table V. Each value is an average of the individual values derived from the pH behavior of the chemical shifts of 8–10 separate protons or carbons. In addition to the chemical shifts of the predominant species at pH ~2, 8, and 14 and pK_{a2} and pK_{a3}, data are also listed for the coupling constant between ^{195}Pt and specific ligand protons and carbons for which platinum satellites are resolved; protonation shifts (shift of protonated species − shift of conjugate base) are also given in Table I.

Figures 6 and 7 are separate plots of chemical shifts vs pH for bpy and tach protons of **1**. The graphs include both experimental data and the curves calculated for each resonance from the five parameters (three shifts and two pK_a values), which are listed in Table I. The same average values for pK_{a2} (5.47) and pK_{a3} (11.74) were used to generate all of the calculated curves. Figures 8 and 9 are similar separate plots of ^{13}C shifts for bpy and tach portions of **1**, with calculated curves based on pK_{a2} = 5.66 and pK_{a3} = 12.10.

Average pK_a values obtained in this way in different experiments are listed in Table V. Though the temperature of all of the samples at the time of pH and NMR measurements was not carefully regulated or even known with certainty, all pH data correspond to 22 ± 3 °C, nominal room temperature in the labs where the measurements were made. The systematic differences between the pK_a values derived from ^{13}C shifts and the values derived from ^{1}H shifts can be attributed mainly to the solvent difference: the ^{1}H data were all obtained with D_2O solutions, while the ^{13}C data were all obtained with 90% H_2O/D_2O solutions, but the pH electrodes were both standardized with buffers in H_2O solvent so a systematic difference in results is expected.[11] In addition, since ^{13}C spectra were proton broad-band decoupled, these solutions may have been maintained at a slightly higher temperature than their ^{1}H counterparts. The excellent agreement between measurements made at different times and at different NMR frequencies suggests that the results are quite reliable.

Determination of pK_a Values: Spectrophotometric Method for pK_{a2} and pK_{a3}. These values were determined from the absorption spectra of a series of solutions whose total platinum concentrations were equal, but whose pHs varied over a 2–3 pH unit range surrounding the pK_a. Pertinent spectral data are summarized in Table II. Since the spectra showed three isosbestic points in the region of maximum absorption, the spectral changes at several different wavelengths were great enough to calculate pK_a values from the data. Like the NMR chemical shift, the absorbance at each wavelength, A, is a weighted average of contributions from acid and conjugate-base forms; i.e.

$$A = (f_{HA}A_{HA}) + (f_{A^-}A_{A^-}) \qquad (7)$$

where A_{HA} and A_{A^-} are the absorbancies of acid and conjugate-base forms at a given total concentration and the fractional populations are given by (5) and (6). Thus, a plot of A vs pH yields a sigmoidal curve with an inflection point at pH = pK_a. In practice, pK_a values were obtained by a least-squares fit of the absorbance–pH data to eq 7, using six to eight data points at each wavelength and A values from the spectra of the stock solutions containing a single species. The pK_a values at 25 °C and ionic strength 0.10 M, obtained in this way, are summarized in Table III. The average values, based on measurements at three different wavelengths, are compared with values from NMR data in Table V.

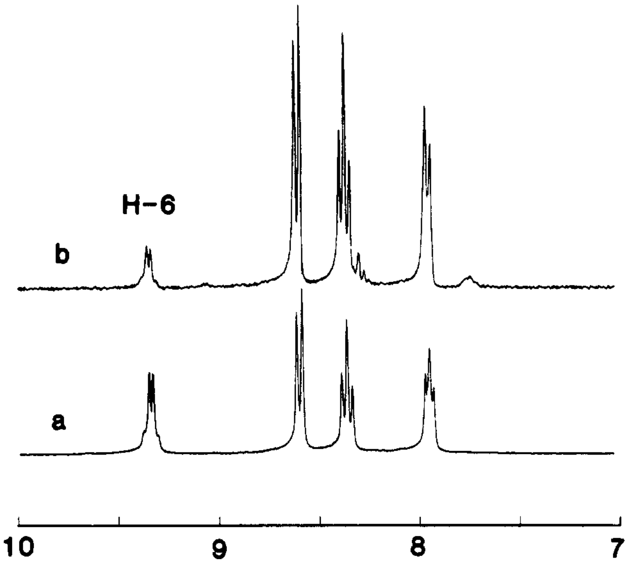

Figure 2. Bipyridyl portion of 300-MHz proton NMR spectrum of **1** in 0.19 M NaOD, showing exchange of H-6 at 60 C: (a) t = 0; (b) t = 1.6 h. Note evidence of partial decomposition in peaks at 8.3 and 7.7 ppm.

Protonation Sites for pK_{a2} and pK_{a3}. The effects of pH on the chemical shifts of the ligand protons and carbons that are shown in Figures 6–9 and in Table I indicate clearly that the two protonation sites with approximate pK_a = 5 and 12 are the two in-plane nitrogens of the coordinated tach. With some significant exceptions, most proton shifts move toward higher frequencies (less shielding) as the pH is decreased and ligand protons are added. Protonation shifts, defined as $\delta_{HA} - \delta_{A^-}$ and listed in Table I for of all protons and carbons, are generally greater for tach protons than for bpy protons. More importantly, the protonation shift is substantially greater for Hα2 than for Hα1, which rules out significant deprotonation at the out-of-plane tach nitrogen in the pH 1–14 range. Carbon-13 shifts provide even more convincing evidence of in-plane nitrogen protonation. Though bpy carbon shifts are not particularly revealing, the large negative (increased shielding) protonation shifts observed for Cβ1 (−5.98 and −5.30 ppm), which lies two bonds from each of the two in-plane nitrogens, correspond closely to the protonation shifts observed for the β-carbon in a large sample of amines (e.g., successive deprotonations shifts of −5.28 and −5.32 ppm are observed for the β-C in 1,3-diaminopropane).[12] Finally, the unusual pattern in the pH dependence of the shifts of the H-6 of bpy and Hβ1 protons also suggests that the protonation sites are near these protons. These patterns will be examined more closely in connection with the H-6 proton-exchange kinetic data as evidence for the orientation of the lone pair of the predominant species at different pHs.

Determination of pK_a Values: pK_{a1} from ^{195}Pt Chemical Shift Data at Low pH. Since no further shifts in UV or NMR spectra are observed between about pH 3 and 1, the pK_a of the most acidic proton must be <0; i.e., the proton must be quite acidic. Since ^{195}Pt chemical shifts cover such a wide range,[13] and since the most acidic protonation site appeared to be that of coordinated water, the effect of 1 M HCl on the ^{195}Pt chemical shift was examined in the hope of detecting a measurable protonation shift for the complex at this concentration of H$^+$.

The ^{195}Pt chemical shifts of **1** at several different pHs and in 1.2 M and 0.6 M DCl are given in Table IV. The ^{195}Pt protonation shifts associated with pK_{a2} and pK_{a3} at pH 5 and 12 are 150 and

---

[11] Bates, R. G. *Determination of pH: Theory and Practice*; 2nd ed.; John Wiley and Sons: New York, 1973; p 375.

[12] Sarneski, J. E.; Suprenant, H. L.; Molen, F. K.; Reilley, C. N. *Anl. Chem.* **1975**, *47*, 2116.

[13] Pregosin, P. S. In *Annual Reports on NMR Spectroscopy*; Mooney, E. F., Ed.; Academic Press: New York, 1986; Vol. 17, p 285.

Table I. Chemical Shifts in ppm from TMS of Basic Forms of **2** and of $[Pt(bpy)(tach)Cl]^{3+}$ [a]

carbon or proton of **2**	$\delta(+3)$	$\delta(3-2)$[b]	$\delta(+2)$	$\delta(2-1)$[b]	$\delta(+1)$	$\delta(Pt-Cl^{3+})$
C-2	155.57 (16)[c]	0.44	155.13	−0.16	155.29 (12)	155.48 (17)
C-3	128.57 (18)	1.59	126.98 (17)	0.87	126.11 (15)	128.91 (18)
C-4	146.82 (<7)	1.70	145.12 (<5)	1.31	143.81 (<5)	146.83 (<6)
C-5	131.31 (25)	1.55	129.76 (21)	0.92	128.84 (17)	131.64 (23)
C-6	149.74 (14)	1.75	147.99 (9)	0.57	147.42 (<10)	149.78 (13)
Cα2	43.93 (17)	−1.33	45.26 (20)	−0.86	46.12 (22)	43.12 (16)
Cα1	41.86 (16)	−0.40	42.26 (20)	−0.03	42.29 (22)	42.41 (15)
Cβ1	31.38 (<10)	−5.98	37.36 (8)	−5.43	42.79 (<10)	31.54 (<10)
Cβ2	31.82 (13)	−1.78	33.60 (16)	−1.75	35.35 (14)	31.25 (15)
H-3	8.834	0.114	8.720	0.075	8.645	8.800
H-4	8.672	0.159	8.513	0.095	8.418	8.637
H-5	8.175	0.083	8.092	0.071	8.021	8.152
H-6	9.295 (21)	−0.270	9.565 (20)	0.181	9.384 (18)	9.220 (22)
H-α2	3.344 (49)	0.706	2.638 (53)	0.440	2.198 (60)	3.184 (45)
H-α1	3.067 (33)	0.225	2.842 (44)	0.171	2.671 (54)	3.059 (47)
H-β1e	2.636	−0.006	2.642	−0.070	2.712	2.612
H-β1a	2.532	0.317	2.215	0.209	2.006	2.449
H-β2e	2.515	0.197	2.318	0.143	2.175	2.537
H-β2a	2.237	0.191	2.046	0.193	1.853	2.235

[a] Calculated from regression analysis of δ vs pH for about 10 points near pK_a. $\delta(+3)$ corresponds to $[Pt(bpy)(tach)CH]^{3+}$, etc. Larger values correspond to less shielding. $Pt-Cl^{3+}$ corresponds to the species $[Pt(bpy)(tach)Cl]^{3+}$ from a solution in 0.18 M DCl. [b] Protonation shift = shift of protonated species − shift of conjugate base. [c] Values in parentheses are coupling constants in Hz between specific C or H and the central ^{195}Pt.

Table II. UV Absorption Data for $[Pt(bpy)(tach\text{-}2H)(H_2O)]Cl_2$ as a Function of pH

pH	predominant species	λ_{max}/nm	$10^4\epsilon/M^{-1}\ cm^{-1}$
3.3	$[Pt(bpy)(tach)OH]^{3+}$	323	1.24
		310	1.11
8.1	$[Pt(bpy)(tach\text{-}H)OH]^{2+}$	316	1.38
		304	1.24
13.2	$[Pt(bpy)(tach\text{-}2H)OH]^{+}$	311	1.58
		299	1.51

Table III. pK_a Values for **2** Derived from UV Spectral Data

λ/nm	pK_{a2}	λ/nm	pK_{a3}
323	5.25	316	11.87
316	5.39	311	11.60
304	5.34	271	11.57
means	5.33 ± 0.05		11.68 ± 0.13

Table IV. Platinum-195 Chemical Shifts[a] of Solutions of $[Pt(bpy)(tach\text{-}2H)(H_2O)]Cl_2$ as a Function of pH or Molar Concentration of DCl

pH	[DCl]/M	δ/ppm	principal species	approx %
12.8		−238	$[Pt(bpy)(tach\text{-}2H)OH]^{+}$	90
7.4		−144	$[Pt(bpy)(tach\text{-}H)OH]^{2+}$	99+
4.2		9	$[Pt(bpy)(tach)OH]^{3+}$	95
1.6		11	$[Pt(bpy)(tach)OH]^{3+}$	99+
	0.6	24	$[Pt(bpy)(tach)OH]^{3+}$	90
	1.2	38	$[Pt(bpy)(tach)OH]^{3+}$	80

[a] In ppm from external 0.2 M Na_2PtCl_6/D_2O.

Table V. Summary of pK_a Values of $[Pt(bpy)(tach)(H_2O)]^{4+}$ at 22 ± 3 °C

pK_a	value		basis	solvent	temp/°C	ion strength
pK_{a1}	−0.6	0.1	Pt NMR	D_2O	room	≈1
pK_{a2}	5.47	0.07	^1H NMR	D_2O	room	≈0.05
	5.66	0.03	^{13}C NMR	H_2O (90%)	room	≈0.05
	5.33	0.05	UV	H_2O	25	0.10
pK_{a3}	11.74	0.05	^1H NMR	D_2O	room	≈1
	12.10	0.06	^{13}C NMR	H_2O (90%)	room	≈0.05
	11.68	0.13	UV	H_2O	25	0.10

100 ppm, respectively. Since these dissociations involve amine protons directly attached to the platinum atom, the dissociation of the coordinated water molecule might also be expected to produce a similar shift. On the basis of the shifts between pH 4.2 and 0.6 M DCl (13 ppm) and between pH 4.2 and 1.2 M DCl (27 ppm), an approximate K_{a1} can be calculated. Assuming a 125 ppm protonation shift, one calculates about 20% protonation in the presence of 1 M excess H^+ $K_{a1} \approx (0.8)(1)/(0.2) = 4$, and p$K_{a1} \approx -0.6$ for the most acidic proton, that of the coordinated water molecule; on the basis of the 0.6 M DCl data, $K_{a1} = 5$. Additional evidence for the protonation of the OH site in HCl is provided by the reaction of **1** with aqueous DCl at low pH.

Rate and Equilibrium Data for the Chloride Anation Reaction of 1. In investigating the bipyridyl H-6 proton exchange as a function of pH, we prepared one sample of **1** in 0.18 M DCl. That sample showed no H-6 proton exchange over several days, even at 60 °C. However, at 60 °C, the proton NMR spectrum showed a clean reaction from starting material to a product whose spectrum was almost identical with that of **1**, except for the chemical shift of the H-6 protons of coordinated bpy and the Hα2 protons of the coordinated tach. On that basis and on the basis of equilibrium calculations which follow, we conclude that the reaction in DCl is the conversion of 1 to the corresponding chloro species, $[Pt(bpy)(tach)Cl]^{3+}$. The peaks associated with **1** decrease exponentially as shown in Figure 5. A nonlinear least-squares fit of the data to the first-order decay expression

$$[Pt\text{-}OH] = [Pt\text{-}OH]_\infty + ([Pt\text{-}OH]_0 - [Pt\text{-}OH]_\infty)e^{-kt} \quad (8)$$

where Pt–OH denotes the Pt–OH species, yielded a value of $(3.8 \times \pm 0.4) \times 10^{-6}\ s^{-1}$ for k, the first-order rate constant at 60 °C.

On the basis of the relative peak heights at equilibrium at room temperature, about 90% of the chloro species, denoted Pt–Cl, is produced and about 10% of the aqua species, denoted Pt–OH at this pH, remains. On the basis of these quantities, the equilibrium constant, K_6, for the reaction

$$Pt\text{-}OH + H^+ + Cl^- = Pt\text{-}Cl + H_2O \quad (9)$$

is on the order of $(10/1)/(0.2)^2 = 10^3/4$. But K_6, given by

$$K_6 = [Pt\text{-}Cl]/[Pt\text{-}OH][H^+][Cl^-] \quad (10)$$

is just $10K_{a1}K_h$, where K_h, the hydrolysis constant for the chloro complex, is

$$K_h = [Pt\text{-}OH_2^+][Cl^-]/[Pt\text{-}Cl] \quad (11)$$

Therefore, $K_h = 1/K_6K_{a1} \approx 1/[(10^3/4) \times 4] \approx 10^{-3}$. This value is typical of hydrolysis constants of chloro complexes of platinum(IV).[14] The first-order kinetics can be accounted for by the fact that a large excess of Cl^- is present. The substitution probably proceeds by a dissociative mechanism involving the small fraction

---

(14) Hartley, F. R. *The Chemistry of Palladium and Platinum* John Wiley and Sons: New York, 1973; p 284.

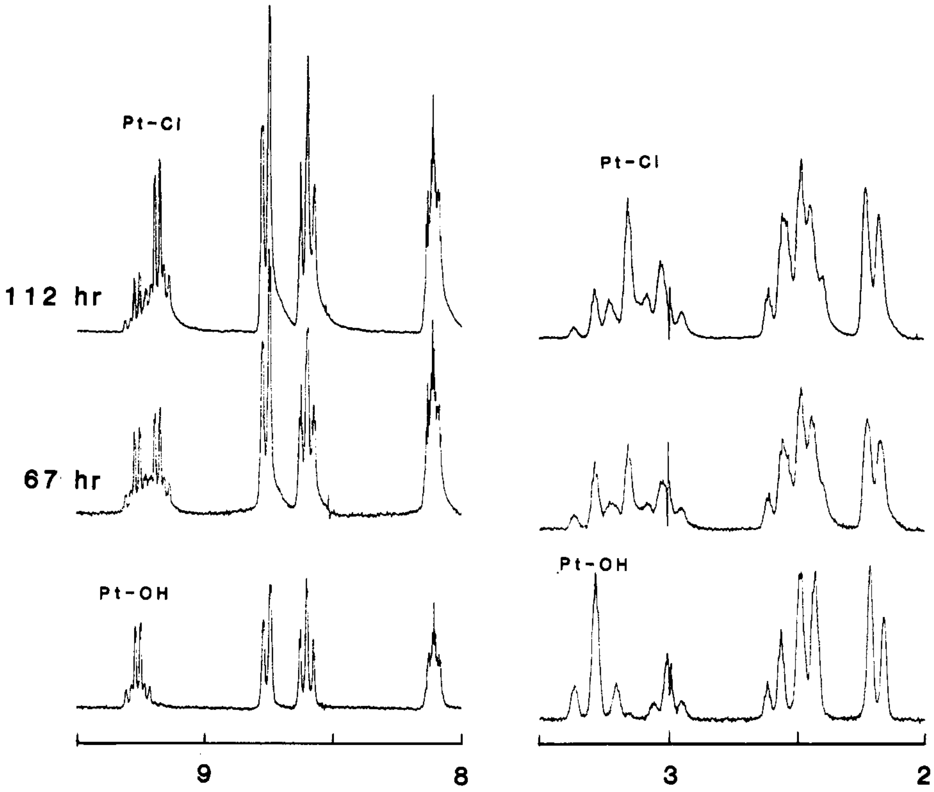

Figure 3. 300-MHz proton NMR spectrum of **1** in 0.18 M DCl/D_2O showing conversion to the chloro species at 60 °C.

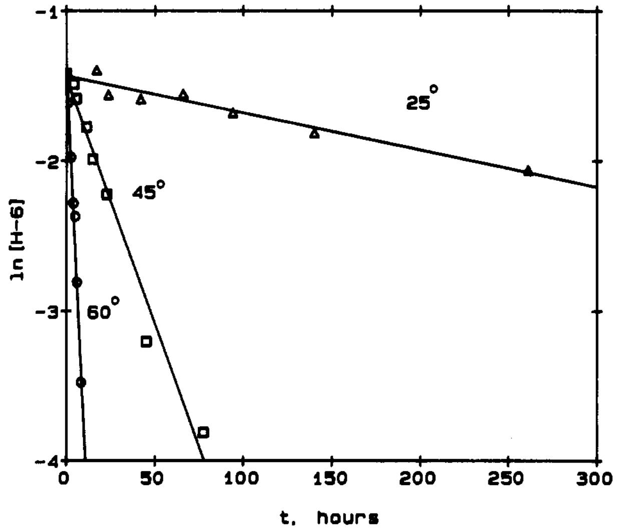

Figure 4. First-order plots of ln [H-6] of **1** vs time at 60, 45, and 25 °C for deuterium exchange in 0.19 M NaOD.

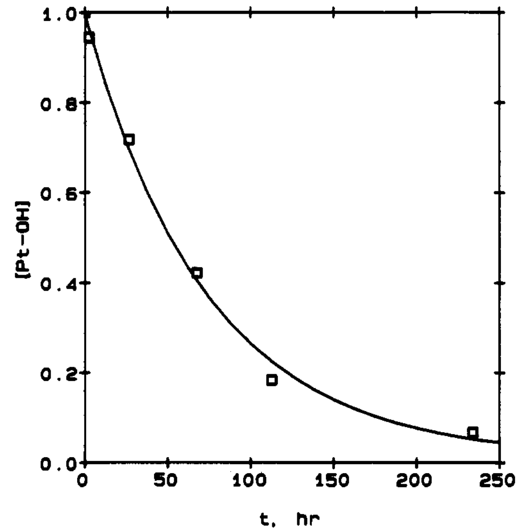

Figure 5. First-order chloride anation of **1** in 0.18 M DCl at 60 °C. The least-squares regression curve of [Pt–OH] vs time is given by 0.011 + 0.985 exp(−0.0136*t*) corresponding to $k_1 = 3.8 \times 10^{-5}$ s^{-1}.

of **1** that is protonated (in the form of $[Pt(bpy)(tach)(H_2O)]^{4+}$) in the 0.18 M DCl solution.[15]

Taken together, these results show clearly that the low-pH protonation and the low-pH reaction with chloride ion involve the coordinated water, which is present mainly as OH except under very acid conditions. The kinetic data are also important because they show that the chloride anation reaction is too slow at room temperature to affect the ^{195}Pt chemical shift measurements made on freshly prepared solutions of **1** in 1.2 M DCl or 0.6 M DCl. These measurements were the basis of the estimate of $K_{a1} \approx 4$. The ^{195}Pt chemical shift for $[Pt(bpy)(tach)Cl]^{3+}$ in 0.18 M DCl is −379 ppm, nearly 400 ppm from the shift for the coordinated hydroxy complex present at this pH.

Kinetics of H-6 Proton Exchange of Coordinated Bpy. First-order rate constants for deuterium exchange of H-6 protons under

Table VI. Effect of pH and Temperature on First-Order Rate Constants[a] for Deuterium Exchange of H-6 of $[Pt(bpy)(tach\text{-}H)(OH)]Cl_2$

pH	[NaOH]/M	*t*/°C	$10^5k/s^{-1}$
	0.19	60	6.6 ± 0.3
	0.095	60	5.5 ± 0.2
	0.042	60	5.3 ± 0.5
	0.19	45	0.91 ± 0.12
	0.19	25	0.069 ± 0.006
8.8		60	0.49 ± 0.03
7.8		60	0.42 ± 0.06
9.2		45	0.12 ± 0.01
8.8		45	0.15 ± 0.01
8.1		45	0.081 ± 0.006
9.2		25	0.010 ± 0.005
8.1		25	0.008 ± 0.002

[a] Each value is based on 5–10 concentration measurements; the standard deviation in *k* is also given.

---

(15) Basolo, F.; Pearson, R. G. *Mechanisms of Inorganic Reactions*, 2nd ed.; John Wiley and Sons: New York, 1967, Chap 4.

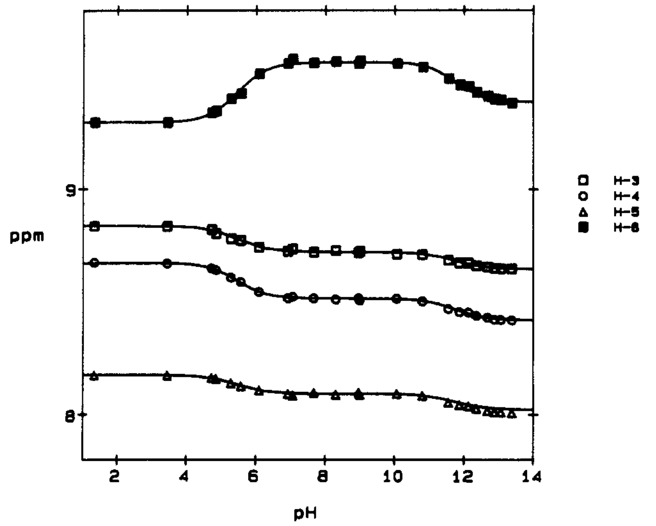

Figure 6. NMR titration of **1**: bpy ligand protons.

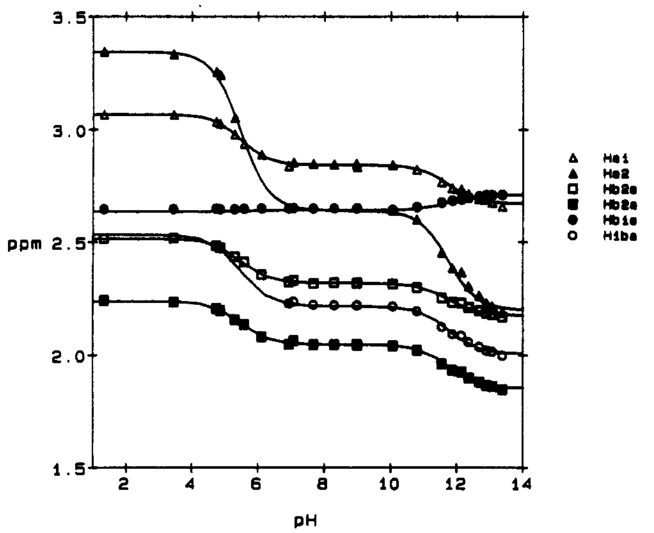

Figure 7. NMR titration of **1**: tach ligand protons.

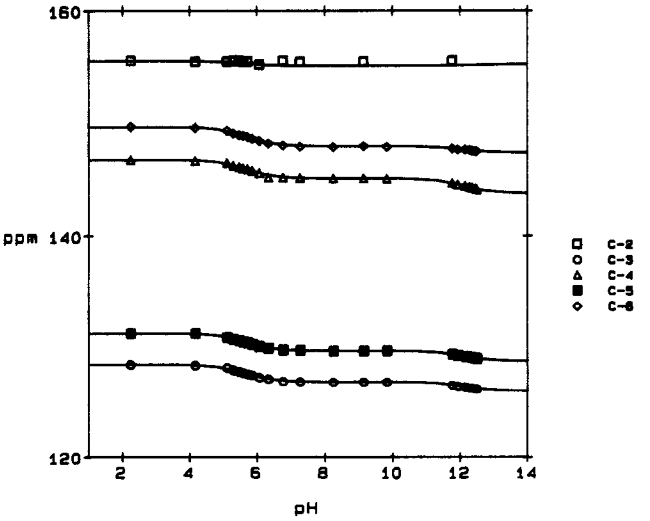

Figure 8. NMR titration of **1**: bpy ligand ^{13}C peaks.

a variety of pH and temperature conditions are listed in Table VI. Several significant conclusions can be drawn from the data: (1) Above pH 12.7 (excess [OH^-] > 0.05 M), where [Pt(bpy)(tach-2H)(OH)]$^+$ is the principal species, the rate of exchange is essentially independent of the concentration of excess OH^-. (2) In the pH 7–9 range, where [Pt(bpy)(tach-H)(OH)]$^{2+}$ is the principal species, the rate of exchange is also independent of pH. (3) The exchange rate in the mid-pH range is only a factor of 10 slower than the exchange rate at high pH at the same temperature. These results suggest strongly that intramolecular catalysis by the proximate basic lone pair(s) of the deprotonated in-plane amine of the tach ligand is responsible for the relatively facile exchange of the H-6 bpy protons.

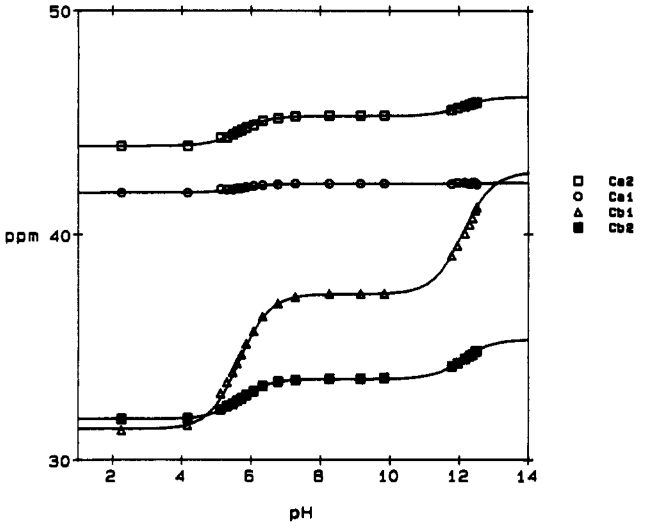

Figure 9. NMR titration of **1**: tach ligand ^{13}C peaks.

Table VII. Activation Parameters for Deuterium Exchange of H-6 of [Pt(bpy)(tach-H)OH]Cl_2

pH	[NaOH]/M	ΔH^{*}/kJ mol^{-1}	ΔS^{*}/J K^{-1} mol^{-1}
	0.19	105 ± 4	56 ± 12
7.8–9.2		91 ± 6	21 ± 18

Table VIII. Comparison of pK_a Values of Structurally Related Species

acid form	conjugate base	pK_a	ref
$Pt(bpy)(tach)(H_2O)^{4+}$	$Pt(bpy)(tach)OH^{3+}$	–0.6	this work
$Pt(bpy)(tach)OH^{3+}$	$Pt(bpy)(tach\text{-}H)OH^{2+}$	5.6	this work
$Pt(bpy)(tach\text{-}H)OH^{2+}$	$Pt(bpy)(tach\text{-}H_2)OH^{+}$	11.6	this work
$Pt(dien)(H_2O)^{2+}$	$Pt(dien)(H_2O)^{+}$	6.1	3, 16
$Pt(gly)(DMSO)(H_2O)^{+}$	$Pt(gly)(DMSO)(OH)$	4.1	4
$Pt(NH_3)_5(H_2O)^{4+}$	$Pt(NH_3)_5OH^{3+}$	4.1	5
$Pt(NH_3)_5Cl^{3+}$	$Pt(NH_3)_4(NH_3)Cl^{2+}$	8.7	6, 7
$Pt(NH_3)_6^{4+}$	$Pt(NH_3)_5(NH_2)^{3+}$	7.9	6, 7
$Pt(en)_3^{4+}$	$Pt(en)_2(en\text{-}H)^{3+}$	5.5	19
$Pt(NH_3)_2(N,N'\text{-}en)^{2+}$	$Pt(NH_3)_2(N,N'\text{-}en\text{-}H)^{+}$	≈16	17
$Pt(bpy)(N,N'\text{-}en)^{2+}$	$Pt(bipy)(N,N'\text{-}en\text{-}H)^{+}$	≈15	17
H_3PO_4	$H_2PO_4^-$	2.2	20
$H_2PO_4^-$	HPO_4^{2-}	7.2	20
HPO_4^{2-}	PO_4^{3-}	12.3	20

Values for activation parameters for H-6 proton exchange, derived from linear plots of ln (k/T) vs $1/T$ based on the Eyring equation, are given in Table VII. The values at high pH, for which the rate constants were more accurately determined, are much more reliable. The reliability of the mid-pH rate data is probably not sufficient to warrant attributing much significance to the small differences between activation parameters at high pH and mid-pH.

Discussion

Comparison of pK_a Values of 2 and Similar Platinum Species. A comparison of pK_a values of **2** and some related platinum species is given in Table VIII. First of all, the coordinated water of **2** (pK_a = –0.6) is significantly more acidic than the coordinated water of the closely related species [$Pt(NH_3)_5(H_2O)$]$^{3+}$ (pK_a = 4.1).[5] The latter is only about as acidic as the two Pt(II) species cited in Table VIII.[3,4,16] This suggests that the Pt–O bond in

---

(16) Alcock, R. M.; Hartley, F. R.; Rogers, D. E. *J. Chem. Soc., Dalton Trans.* **1973**, 1070.

2 is stronger than the Pt–O bond in the pentaammine complex. This could be related to a weaker Pt–N bond of the axial amine of the coordinated tach relative to the trans NH_3 of the ammine species. However, three-bond Pt–H coupling is not much different for in-plane and out-of-plane Hα protons of the tach moiety of **2**, so the pK difference may be the result of the difference between two cis pyridine vs two cis NH_3 ligands. Of the two similar platinum(II) complexes with N,N'-dimethylethylenediamine (N,N'-dmen), the bpy complex is more acidic than the $(NH_3)_2$ species.[17] $[Pt(bpy)(H_2O)_2]^{2+}$ also appears to be several orders of magnitude more acidic than *cis*-$[Pt(NH_3)_2(H_2O)_2]^{2+}$.[18]

The first pK of the coordinated tach of **2** (pK_a = 5.5) is comparable to pK values for other coordinated amines in highly charged cationic Pt(IV) species.[5,7,19] However, dissociation of the first proton of $Pt(en)_3^{4+}$ should be expected to be greater than pK_{a2} for **2**, since the latter represents the dissociation of a 3+ species. So the effect of bipyridine appears to be significant in enhancing the acidity of tach protons of **2**.

Not surprisingly, tach protons of **2** are considerably more acidic than comparable amine protons in cationic +2 diamine–bipyridyl Pt(II) species, for which p$K_a \approx 15$.[17] The difference must be attributable to the difference in oxidation states of the central metal. It appears that no attempts have been made to determine the second pK of Pt(IV) species like $Pt(en)_3^{4+}$. In view of the data for **2**, dissociation of a second N–H proton of $Pt(en)_3^{4+}$ in water should be observable below pH 14, and we are currently investigating this possibility further.

The pattern of pK_a values for **2** is strikingly parallel to the pattern for orthophosphoric acid,[20] with one strongly acidic site, a second weakly acidic site (with pK = 5–7), and a third very weakly acidic site. The increment in pK_a between sites for **2** is about 6 (–0.6 to 5.5 to 11.7); for orthophosphoric acid, about 5 (2.2 to 7.2 to 12.3). The tach species, **2**, starts out as a +4 cation that loses positive charge with each dissociation, while phosphoric acid starts out as a neutral species that becomes more negatively charged with increased dissociation. However, for both species, the three acidic sites are on adjacent atoms that are bound to a central atom in its highest oxidation state, so the comparison seems appropriate.

From the structural point of view, species **2** strongly resembles the monomeric species $[Pt(bpy)(CH_3)_3(H_2O)]^+$ (**6**), which Clegg, Hall, and Ham[21] prepared from tetrameric trimethylplatinum(IV) iodide via $[Pt(CH_3)_3(H_2O)_3]_2SO_4$. Though no attempt was made to determine the pK_a of the trimethyl-bpy species, the evidence was strong that the water site was protonated under the conditions of their investigation. In D_2O solutions of **6**, they were able to observe the coalescence of the proton NMR signals of in-plane (two methyls) and out-of-plane (one methyl) CH_3 groups below 100 °C, and they attributed this coalescence to the facile loss of coordinated water to yield a fluxional 5-coordinate intermediate which readily interconverts in-plane and out-of-plane methyl groups. We have seen no evidence for a similar equilibration of in-plane and out-of-plane amines of coordinated tach in **2**. Since the chloride anation most likely proceeds by a dissociative mechanism, the rate of anation would be a measure of the rate of water loss. In view of the slugishness of the anation reaction at 60 °C, it does not seem likely that coalescence below 100 °C would be observed for **2**, even for solutions in which the water site is fully protonated. So, it is not surprising that the pK_a of the single potentially acidic site of **6**, with a weakly bound water, is considerably greater than that of **2**.

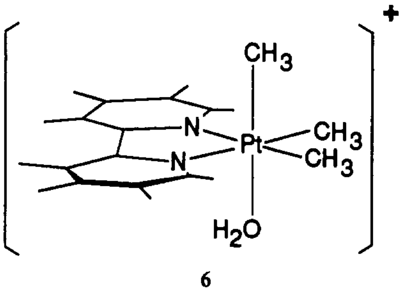

6

Structures of Mid-pH and High-pH Forms of 2. Both NMR and kinetic data provide evidence regarding the structural details of the 2+ and 1+ forms of **2** that predominate in the pH 7–10 and >13 regions, respectively. As shown in Figures 6 and 7, the pH dependence of the proton chemical shift for H-6 of the bpy fragment and H-β1e of the tach fragment is unusual. Most of the other protons shift monotonically toward increased shielding while the carbons shift toward decreased shielding with increased pH as protons are successively removed. Furthermore, the increment in shift is about the same for removal of each proton. However, for the H-6 and H-β1e sites, the overall shift between pH 3 and 13 corresponds to decreased shielding. More importantly, the increment per proton removed is not equal for the two steps. In fact, removal of the first tach proton produces a substantial decrease in shielding for the bpy H-6, which is not entirely compensated by the increase in shielding for removal of the second proton. The two protons of **2** that show unusual chemical shift behavior are just the two protons that are closest to the in-plane nitrogen deprotonation sites.

A plausible explanation for the unusual behavior of H-6 and H-β1e can be found in examination of the detailed stereochemistry of the deprotonated species. As shown in Figure 1, the lone pair of the deprotonated in-plane NH_2 of coordinated tach can occupy either axial or equatorial sites in the chair conformation of the six-membered Pt-containing ring. Between pH 7 and 10, where the 2+ species (with one lone pair on an in-plane tach nitrogen) predominates, two isomers are possible; these are denoted eH and aH, respectively. However, at high pH, where both in-plane nitrogens are deprotonated, three isomers are possible; these are denoted ae or ea, ee, and aa. Proton transfer would be expected to interconvert the two (pH 7–10) or three (high-pH) species rapidly on an NMR time scale so that the chemical shifts calculated for each protonation state would be average values of the shifts of the individual species. If the same ratio of axial to equatorial orientations prevailed for both 2+ and 1+ species, the chemical shift increment per proton removed should be roughly equal for protons nearest the deprotonation sites, H-6 and H-β1e. At the very least, the shifts should be in the same direction. The unusual pattern shown by the effect of pH on the shifts of these protons then suggests a substantial change in the ratio of axial/equatorial orientations between **4** and **5**, species having one and two deprotonated amine groups, respectively.

The effect of pH on the rate of H-6 proton exchange provides an important clue to the direction of the shift in the axial–equatorial ratio with pH. The lack of specific hydroxide ion concentration dependence for the rate, even at high pH, requires an intramolecular catalysis of the exchange reaction by a lone pair of electrons of deprotonated tach. Inspection of molecular models reveals that an equatorial orientation for the lone pair *is required* for the increased polarization of the $C–H_6$ bond that is necessary for the facile H-6 exchange in D_2O. In the absence of any other effects, if the fraction of lone pairs with an equatorial orientation were the same for both mid- and high-pH species, the rate of H-6 exchange might be expected to double when the second proton is removed. In fact, the rate at high pH is about a factor of 10 greater than the rate at mid-pH. While this observation suggests that the high-pH form contains a much higher fraction of equatorially oriented lone pairs than the mid-pH form, other evidence can be invoked that leads to the opposite conclusion.

In attempting to connect the rate of H-6 proton exchange to the orientation of the lone pair on nitrogen, two factors need to be considered: the orientation of the lone pair and the basicity of the lone pair. For the doubly deprotonated 1+ species at high

---

(17) Erickson, L. E. *J. Am. Chem. Soc.* **1969**, *91*, 6284.
(18) Wimmer, S.; Castan, P.; Wimmer, F. L.; Johnson, N. P. *J. Chem. Soc., Dalton Trans.* **1989**, 408.
(19) Jørgensen, C. K. *Acta Chem. Scand.* **1956**, *10*, 518.
(20) Smith, R. M.; Martell, A. E. *Critical Stability Constants*; Plenum Press: New York, 1976; Vol. 4.
(21) Clegg, D. E.; Hall, J. R.; Ham, N. S. *Aust. J. Chem.* **1970**, *23*, 1981.

pH, $pK_b \sim 2$. In contrast, for the singly deprotonated mid-pH 2+ species, $pK_b \sim 8$. For each species, the deprotonated coordinated amino groups are the most basic centers. With a difference of about 6 in pK_b, the lone pair of the high-pH form would be expected to be a much better catalyst for the H-6 exchange reaction. Classical linear free energy considerations would lead to the expectation of a large increase in the effectiveness of the more basic form (perhaps 10^3, or more) in catalyzing deuteration of H-6.[22] This leads to the conclusion that the rate of exchange of the mid-pH 2+ species is unusually fast (though actually a factor of 10 slower) relative to the high-pH 1+ form, which is much more basic. Furthermore, the H-6 chemical shift data require that the fractional population of the preferred orientation of the tach lone pair(s) changes substantially in going from singly deprotonated (2+) to doubly deprotonated (1+) species. For example, a shift from 2% to 10% equatorial orientation between mid- and high-pH forms cannot explain the H-6 chemical shift data. Taken together, these data indicate that the axial–equatorial (ae) or diaxial lone-pair species (aa) predominates for the doubly deprotonated high-pH form, while the equatorial lone-pair species (eH) predominates for the singly deprotonated mid-pH form. In any event, the data for the high-pH species are not compatible with the ee species dominating.

Two other observations support the conclusion that the single lone pair of the 2+ species prefers the equatorial orientation. The decreased shielding observed for H-6 when the 3+ species loses a proton to form the 2+ species is the only shift seen in this direction for all the bpy protons with addition of base (Figure 6). This highly unusual behavior could be accounted for on the basis of substantial interaction between H-6 and the equatorial lone pair of the 2+ eH species. Such behavior is analogous to the decreased shielding associated with hydrogen bonding.[23] In addition, the H-α2 proton signal and the H-6 proton signal of the 2+ species show extensive, field-dependent broadening over the whole pH range where the 2+ species is the principal species (from pH 6 to 10). Complete averaging of the environment of axial and equatorial orientations of the two in-plane nitrogen sites required to average the magnetic environments of the two H_6 and two $H\alpha 2$ protons requires more than simple nitrogen inversion. Multiple proton transfers via symmetric 1+ or 3+ species or proton transfers in combination with lone-pair inversions are required. A relatively favorable interaction between H-6 and the equatorially oriented lone pair of the adjacent tach nitrogen could be responsible for slowing these processes to the point that extensive broadening is observed in the 2+ species.

Finally, the conformational preference of a proton vs a lone pair of nitrogen in saturated heterocyclic nitrogen compounds, investigated by a variety of techniques, provides some evidence to support our conclusions about the structures of deprotonated tach. On the basis of NMR evidence, Sudmeier and Occupati concluded that the proton and the lone pair have comparable preferences for the axial orientation in substituted piperazines.[24] Katritzky and co-workers concluded that the N–H equatorial (lone pair axial) conformation predominates in piperidine by about 2:1 (0.4 kcal mol^{-1}) at room temperature.[25,26] These results suggest that the axial/equatorial preference of the proton and the lone pair on nitrogen is small enough that intramolecular structural features of the complex can be expected to have substantial effects on the relative population of axial and equatorial forms for the deprotonated NH_2 fragments of coordinated tach.

Consideration of the bonding in these pseudooctahedral platinum(IV) complexes may provide some insight into the apparent reversal in the stereochemical preference of the aminate lone pairs in **4** and **5**. According to molecular orbital arguments, a d^6 octahedral complex will place the metal d electrons into t_{2g} orbitals (π bonding). The d^6 metal ion and its ligands can participate in ligand-to-metal π back-bonding as has been invoked to account for the weak-field spectrochemical series behavior of, for example, fluoride ion in CoF_6^{3-}.[27] Highly charged Pt(IV) might be expected to show some tendency to accept π-back-bonding electron density from its ligands. The t_{2g} π orbitals (d_{xy}, d_{yz}, d_{xz}) of the metal ion could form substantial π overlap with filled pure p orbitals on the σ-bound ligands, accepting electrons into π-antibonding MOs.

In the 1+ complex, **5**, the coordinated hydroxide ion could be thought to contribute π density in such a fashion to the platinum center using its p orbital and the metal d_{yz} orbital. The fact that hydroxide is a stronger base than H_2O, but is a weaker ligand in the spectrochemical series than water, may be attributed to this kind of π-donation interactions.[28] In the 2+ complex with one coordinated NH^-, the nitrogen lone pair prefers the equatorial environment on the chair chelate ring pointing toward the bpy H-6. This lone pair could possibly π bond to the in-plane d_{xy} orbital of the metal, but if approximate sp^3 hybridization is maintained at the nitrogen center, the lone pair does not find itself in the appropriate pure p orbital to π bond optimally.

The chair structure of the six-membered 1,3-diamine metal chelate rings have been found to exhibit certain characteristic distortions due to the long M–N bonds and small chelate N–M–N angle ($\sim 90°$):[29,30] (1) a flattening of the chair structure in the region of the dihedral angle formed by the NMN and the NCCN planes to a value much less than the ideal 60° of cyclohexane and (2) opening up of the M–N–C_α angle to a value near 120°, instead of the 109° found for pure tetrahedral hybridization of the N donor atom. The crystal structure of the tach complex, **1**, shows M–N–C_α bond angles of 117° for the in-plane ring (Pt–N–$C_{\alpha 2}$) and 116° for the apical nitrogen.[31] The rigidity of the facial binding ligand restricts the flattening that the chain chelate rings can achieve in **1**. On the other hand, the analogous 1,3-diaminocyclohexane chelate shows both of these distortions.[31]

Since the bond angle of the Pt–N–$C_{\alpha 2}$ in **1** is nearly 120°, it might be possible for the nitrogen lone pair to be viewed as being in a nearly pure p orbital. Such an arrangement would be expected to render the lone pair much less basic than a similar sp^3 lone pair. However, in view of the internally catalyzed bpy H-6 exchange observed for **4**, an equatorial orientation of the lone pair in an sp^3-like hybrid orbital is indicated.

Removal of the third acidic proton of **2** from the second in-plane nitrogen, at $pK_{a3} \sim 11.6$, occurs quite readily by comparison with other platinum(IV) complexes. This basic lone pair does not seem to prefer an equatorial orientation like its counterpart in **4**. A predominantly axial sp^3 lone pair could help to explain the unexpectedly small increase in deuteration rate seen between the pHs where **4** and **5** are the predominant species. An alternative explanation may involve π bonding of this second deprotonated amine group to the platinum center, with the nitrogen atom being $\sim sp^2$ hybridized and the lone pair being in a nearly pure p orbital to maximize π interaction. This amine lone pair would then contribute little to the deuteration of the bpy H-6, except perhaps to enhance the basicity of the sp^3-hybridized lone pair on the other nitrogen. Why the first formed deprotonated amino group would behave so differently in terms of π bonding is not readily apparent to us at this moment.

Some support for the different π bonding of the deprotonated amine groups of **4** comes from the crystal structure of **1**, which, like **4**, has two deprotonated in-plane nitrogen atoms. One of the amine groups uses all of its hydrogen-bonding capability while the other exhibits none. If the latter nitrogen had its lone pair

---

(22) Isaacs, N. S. *Physical Organic Chemistry*; Longman Scientific and Technical: Essex, England, 1987; Chapter 9.

(23) Harris, R. K. *Nuclear Magnetic Resonance Spectroscopy: A Physicochemical View*; Pittman Publishing Inc.: Marshfield, MA, 1983; p 199.

(24) Sudmeier, J. L.; Occupati, G. *J. Am. Chem. Soc.* **1969**, *90*, 154.

(25) Blackburne, I. D.; Katritzky, A. R.; Takeuchi, Y. *J. Am. Chem. Soc.* **1974**, *96*, 682.

(26) Jones, R. A. Y.; Katritzky, A. R.; Richards, A. C.; Wyatt, R. J.; Bishop, R. J.; Sutton, L. E. *J. Chem. Soc. B* **1970**, 127.

(27) Huheey, J. E. *Inorganic Chemistry*, 3rd ed.; Harper and Row: New York, 1983; p 430.

(28) Crabtree, R. H. *The Organometallic Chemistry of the Transition Metals*; John Wiley: New York, 1988; p 15.

(29) Jurnak, F. A.; Raymond, K. N. *Inorg. Chem.* **1974**, *13*, 2387.

(30) Van Kralingen, C. G.; Reedijk, J.; Spek, A. L. *Inorg. Chem.* **1980**, *19*, 1481.

(31) Sarneski, J. E.; et al. Unpublished results from ref 1.

π back-bonded to the metal, the lone pair is no longer as prone to hydrogen bonding to a water molecule as the lone pair on the other deprotonated amine group; the 117° Pt–N–$C_{\alpha 2}$ bond angle would make a pure p orbital feasible for the lone pair in the π-bonding process, with the p orbital orientation appropriate to interaction along the z axis. Interestingly, the platinum–bpy nitrogen bond distance, for the bond trans to the non-hydrogen-bonded, deprotonated amino group is significantly longer than the other Pt–bpy N bond, 2.135 (9) vs 2.044 (8) Å. Simultaneous σ and π ligand-to-metal donation might be expected to weaken the bond trans to itself, as reported for $Os(en)(en\text{-}H)_2^{+}$.[32] The Pt–deprotonated amino nitrogen bond postulated to have a significant π-bonding component is slightly shorter than its counterpart, 2.013 (8) vs 2.044 (8) Å; however, this difference is too small to be useful in any argument. Finally, it is of interest to compare the Pt–N(bpy) bond distances in **1** and the analogous platinum(II) complex $[Pt(bpy)(dach)]Cl_2$, where dach = *cis*-1,3-diaminocyclohexane.[1] Surprisingly, both Pt–N(bpy) distances in the latter complex, 1.988 and 2.029 Å, are shorter than the corresponding distances in **1**.

The trends observed in the J_{Pt-H} data for the 3+, 2+, and 1+ series (Table I) are consistent with the deprotonation scheme described. For the tach $\alpha 2$ protons, the coupling of Pt and H increases as the amino groups are deprotonated, a trend to be expected as the electron density at the ligating nitrogen atom is increased. In contrast, for bpy C-5, J_{Pt-C} decreases as the amine protons are removed. Thus, as the tach ligand is deprotonated, it is bound more tightly to the platinum metal ion while the bpy ligand is, concommitantly, less tightly held. Similarly, the value reported for $^3J_{Pt-H}$ for the bpy H-6 of **6** ($[Pt(bpy)(CH_3)_3(H_2O)]^+$), 12 Hz,[21] is considerably smaller than the 20 Hz observed for that coupling in **5**. The very strong bonds between Pt and the methyl carbons in **6** weaken the Pt–N bond of the bpy moiety even more than deprotonation of the amine sites of **2**. Other resonances listed in Table I generally follow this pattern; $C_{\alpha 1}$ is an especially pronounced example, in spite of the fact that the apical nitrogen atom is not at all involved in any acid–base chemistry over the pH range studied.

Contrast between Bpy Proton Exchange of 1 with Bpy Proton Exchange in Tris(bipyridine) Complexes of Ru(II), Os(II), and Rh(III). The relatively facile H-6 proton exchange observed for **1** contrasts sharply with the superficially similar proton exchange reported for $Ru(bpy)_3^{2+}$,[8] $Os(bpy)_3^{2+}$,[9] and $Rh(bpy)_3^{3+}$.[10] Constable has recently reviewed the evidence that bpy proton exchange in all three of these systems involves simple base catalysis by methoxide, even though the H-3 proton is the labile proton for the Ru(II) and Os(II) species, while the H-6 proton is more labile for the Rh(III) species. However, for all three tris(bipyridine) species, very basic conditions are required to observe the exchange. This contrast with our observations on deuterium exchange of bpy H-6 for the tach species emphasizes the critical importance of the stereochemistry of the lone pair (with $pK_{a2} = 5.5$) in catalyzing the facile H-6 proton exchange observed for **1**, even in the mid-pH range. No evidence for bpy H-3 exchange for **1** has been observed.

Related Work in Progress. Further experiments are in progress to establish the specific rate processes that are responsible for the observed broadening of spectral lines observed in the pH 6–10 range where the 2+ species predominates. We have also prepared the 1,4,7-triazanonane analogue of **1** to compare its acid–base and proton-exchange properties with those of **2**. Preliminary experiments suggest similar acid–base properties, but much less facile bpy–proton exchange for the 1,4,7-triazanone compound relative to the tach analogue.

Acknowledgment is made to the donors of Petroleum Research Fund, administered by the American Chemical Society, for support of this research and to the Pew Charitable Trust and the National Science Foundation for support for the NMR and UV spectrometers used in this work at Grinnell College. J.E.S. acknowledges the support of the Research Corp. and the support of the Fairfield University Research Committee. The support of the NIH for the Southern New England High-Field NMR Facility at Yale University is gratefully acknowledged. J.E.S. also wishes to thank the other Fairfield undergraduates who worked on other aspects of the Pt(bpy)(tach) chemistry, including Kimberly A. Lucey, Anne T. Lynch, and W. Stephen Faraci.

---

(32) Lay, P. A.; Sargeson, A. M.; Skelton, B. W.; White, A. H. *J. Am. Chem. Soc.* **1982**, *104*, 6161.